



## Covalent TiO<sub>2</sub>/pectin microspheres with Fe<sub>3</sub>O<sub>4</sub> nanoparticles for magnetic field-modulated drug delivery



Elisangela P. da Silva<sup>a</sup>, Danielly L.A. Sitta<sup>a</sup>, Vanessa H. Fragal<sup>a</sup>, Thelma S.P. Cellet<sup>a</sup>, Marcos R. Mauricio<sup>a</sup>, Francielle P. Garcia<sup>b</sup>, Celso V. Nakamura<sup>b,c</sup>, Marcos R. Guilherme<sup>a</sup>, Adley F. Rubira<sup>a</sup>, Marcos H. Kunita<sup>a,\*</sup>

<sup>a</sup> Department of Chemistry, State University of Maringá, Av. Colombo, 5790, CEP 87020-900 Maringá, Paraná, Brazil

<sup>b</sup> Department of Basic Sciences of Health, State University of Maringá, Av. Colombo, 5790, CEP 87020-900 Maringá, Paraná, Brazil

<sup>c</sup> Graduate Program in Pharmaceutical Sciences, Department of Basic Science of Health, State University of Maringá, Av. Colombo, 5790, CEP 87020-900 Maringá, Paraná, Brazil

### ARTICLE INFO

#### Article history:

Received 7 January 2014

Received in revised form 13 February 2014

Accepted 14 February 2014

Available online 21 February 2014

#### Keywords:

Drug delivery  
Nanotechnology  
Pectin

### ABSTRACT

Covalent TiO<sub>2</sub>-co-pectin microspheres containing Fe<sub>3</sub>O<sub>4</sub> nanoparticles were developed through an ultrasound-induced crosslinking/polymerization reaction between the glycidyl methacrylate from vinyl groups in TiO<sub>2</sub> and in pectin. ζ-potentials became less negative in the nanostructured microspheres, caused by the presence of both inorganic particles in the negatively charged pectin. The nanostructured pectin microspheres showed an amoxicillin release rate slower than that of pure pectin microspheres. The proposed microspheres were found to be a sustained release system of amoxicillin in the acid medium. Furthermore, the antibiotic release may be modulated by exposition of the microspheres to a remote magnetic field. In practical terms, the nanostructured microspheres could deliver a larger proportion of their initial load to specific site of action. The cytotoxic concentrations for 50% of VERO cells (CC<sub>50</sub>), calculated as the concentration required to reduce cell viability by 50% after 72 h of incubation, for pectin-only microspheres and nanostructured pectin microspheres were 217.7 ± 6.5 and 121.5 ± 4.9 μg mL<sup>-1</sup>, respectively. The obtained CC<sub>50</sub> values indicated acceptable cytotoxic levels for an incubation period of 72 h, showing that the pectin microspheres have a great pharmacological potential for uses in biological environments, even after the introduction of both Fe<sub>3</sub>O<sub>4</sub> and TiO<sub>2</sub>.

© 2014 Elsevier B.V. All rights reserved.

### 1. Introduction

In the last years, smart (or intelligent) release systems (also called advanced materials) have been the target of important scientific investigations [1–5], owing to their specific properties of being sensitive to external stimuli, such as temperature, pH and magnetic field. Drug delivery systems based on nanoparticles sensitive to a remotely applied magnetic field appear on the top of the (bio)technological innovations, because the magnetic field, if used in a therapeutic level, does not affect biological tissues.

Magnetite (Fe<sub>3</sub>O<sub>4</sub>) is a type of magnetic particle that has been the target of important studies on biomedicine because of its non-toxicity, high level of accumulation in tissues, interruption of magnetization when the magnetic field is removed, and biocompatibility due to high affinity for water which allows to interact with

biological species [6–8]. The combination of Fe<sub>3</sub>O<sub>4</sub> with naturally occurring materials to produce a smart drug delivery system for use in pharmaceutical formulation is an innovative concept from a biotechnological point of view.

Pectin is an example of naturally occurring material that has received considerable attention in biomedicine [9,10]. The great advantage of using pectin in the development of micro and/or nanoparticles for drug delivery is based on its appealing properties such as biodegradability, controllable biologic activity, and flexible chains that allow the modulation of the polysaccharide to a specific shape. In this connection, pectin is an appropriate material for use in pharmaceutical formulations [11,12]. This polysaccharide has been studied to act as a polymer biodevice for the treatment of some types of cancer that affect specific regions of the gastrointestinal tract (GI), for example, the colon. This is possible because pectin resists the drastic variations of the physiologic pH throughout GI, which assures the integrity of its polymer structure [13–15]. Although the majority of the reports on pectin-based drug delivery systems have been focused on the treatment of GI diseases,

\* Corresponding author. Tel.: +55 44 3011 3686; fax: +55 44 3261 4125.  
E-mail address: [mhkunita@gmail.com](mailto:mhkunita@gmail.com) (M.H. Kunita).

some studies have shown the use of this polysaccharide in mucosa, owing to its mucoadhesive properties [16–19]. However, the high solubility of pectin in water limits its application in a physiological medium, which can contribute to a premature release of the active principle. Chemical modification of pectin by the introduction of hydrophobic groups has been proposed to reduce its solubility. The incorporation of vinyl groups derived from glycidyl methacrylate (GMA) to polysaccharides is a prominent modification strategy [20].

The focus of this work was on developing a smart biodevice based on magnetic pectin microspheres that shows a sustained release profile in a specific site in which the drug plays a role as a local therapeutic agent. The concept of such a device may be based on a tortuosity effect that sustains the release of the drug. This behavior is the result of the disposition of nanoparticles within the polymer device. A way of doing this is to incorporate inorganic nanoparticles to biodevice (pectin microspheres). This new material could be obtained by a pectin microsphere-nanostructuring approach using  $\text{Fe}_3\text{O}_4$  as magnetic particle, and titanium ( $\text{TiO}_2$ ) as an inorganic crosslinker. Such architecture could show a versatile release profile. The release of the drug could be sustained for a longer time, and also controlled remotely. Furthermore, the introduction of  $\text{TiO}_2$  as a crosslinker for modified pectin could produce consistent microspheres. To obtain microspheres, a covalent approach using chemically modified  $\text{TiO}_2$  was developed. This process consisted of inserting vinyl radical onto  $\text{TiO}_2$  structure for further radical reaction with vinylated pectin.

The proposed biodevice is addressed to the treatment of *Helicobacter pylori* (*H. pylori*)-associated ulcers that affect the mucosa of the stomach. Amoxicillin was used in the studies of release because it inhibits the growth of *H. pylori*. This antibiotic is effective against *H. pylori* in the *in vitro* therapy in which low doses of the drug are required over the oral administration. However, to obtain the same efficiency in the *in vivo* therapy, higher doses of the antibiotic are required, owing to the high rate of emptying of food (or contents) from the stomach into intestine that limits the release and absorption of a given drug. The magnetic pectin microspheres are a new architecture that shows a great potential for future tests in the treatment of gastric ulcers.

## 2. Experimental part

### 2.1. Materials

Pectin from citrus peel (Galacturonic acid  $\geq 74.0\%$  – Sigma–Aldrich, CAS 900-69-5), glycidyl methacrylate 97%, (GMA, Aldrich, CAS 106-91), iron (II and III) oxide particles ( $\text{Fe}_3\text{O}_4$ ), powder  $< 5$  micron, 98% (Aldrich), poly(vinyl alcohol) 87–89% hydrolyzed,  $M_w \cong 31.000 \text{ g mol}^{-1}$  (Aldrich), sodium persulfate  $\geq 98\%$ , (Aldrich), benzyl alcohol 99.8% (Fmaia-Brazil), acetone (Fmaia-Brazil), absolute ethanol P.A. 99.5% (Nuclear, Brazil), hydrochloric acid 37% (HCl, Fmaia-Brazil). Dulbecco's modified Eagle's medium (DMEM-Gibco) and fetal bovine serum (FBS) were obtained from Invitrogen (Grand Island, NY, USA).

### 2.2. Insertion of vinyl radical to pectin by GMA reaction

Twelve grams of pectin were dissolved in 480 mL of distilled water at  $60^\circ\text{C}$ . Hydrochloric acid was introduced dropwise until a pH 3.5 was obtained. After the addition of 1.29 g GMA, the formed solution was kept under stirring at  $50^\circ\text{C}$  for 24 h. The final solution was precipitated in ethanol and separated by centrifugation under stirring of 7000 rpm (Sorvallenged XT/XTR) at  $10^\circ\text{C}$ . The obtained product was lyophilized at  $-55^\circ\text{C}$  for 24 h.

### 2.3. Insertion of vinyl radical to $\text{TiO}_2$ by GMA reaction

Hydrochloric acid was added dropwise to 100 mL of a stirred aqueous suspension of  $\text{TiO}_2$  (0.1 g) until pH 3.5 was reached. After the suspension was heated to  $60^\circ\text{C}$ , 330  $\mu\text{L}$  of GMA were introduced under stirring of 1000 rpm. After 12 h of reaction at  $60^\circ\text{C}$ , the product was washed several times with ethanol to remove both residues and impurities and separated by centrifugation under a speed stirring of 7500 rpm at  $10^\circ\text{C}$ . The material was lyophilized at  $-55^\circ\text{C}$  for 24 h.

### 2.4. Synthesis of $\text{TiO}_2$ -crosslinked pectin microspheres with $\text{Fe}_3\text{O}_4$ nanostructure

Five milliliters of water were used to dissolve modified pectin (1% in w/v), PVA (2% in w/v) and 20 mg of sodium persulfate. After the homogenization of the mixture at room temperature, known amounts of  $\text{TiO}_2$  and  $\text{Fe}_3\text{O}_4$ , were incorporated. The 5 mL of the formed solution were poured to 20 mL of benzyl alcohol (proportion of 1:4), resulting in a two-phase system in which the alcoholic portion is the external phase. The water/oil mixture was sonicated with the use of a probe of ultrasonic oscillation (Cole-Parmer® 500, model EW-04711-40), applying a frequency of 20 kHz for 60 s. The product was separated from the emulsion by centrifugation at 7000 rpm, washed with ethanol and acetone (three times in each) to remove both benzyl alcohol and PVA. To illustrate the preparation of  $\text{TiO}_2$ -crosslinked pectin microspheres, a synthesis scheme is shown in Fig. 1.

To identify the different compositions of the microspheres, the following notation was used to label the samples:  $\text{PM}_x\text{T}_y$ , where P, pectin; M,  $\text{Fe}_3\text{O}_4$ ; x, amount of  $\text{Fe}_3\text{O}_4$ ; T,  $\text{TiO}_2$ , and y, amount of  $\text{TiO}_2$ . The amounts of  $\text{TiO}_2$  and  $\text{Fe}_3\text{O}_4$  were given in mass percentage with respect to weight of modified pectin.

### 2.5. Release of amoxicillin from the microspheres in an acid environment

The amoxicillin was encapsulated into the microspheres using an *in situ* drug loading approach. For this purpose, the antibiotic was introduced to the microsphere-forming emulsion (described above) to be encapsulated during the synthesis. The amoxicillin mass corresponded to 10% of the pectin mass used in the microsphere synthesis. The amount of encapsulated amoxicillin was determined by spectrophotometry at 228 nm, which is the wavelength for the maximum absorption of the antibiotic. The values were determined by the difference between the initial antibiotic mass and the antibiotic mass in the supernatant of the microsphere-forming emulsion.

One hundred milligrams of amoxicillin-loaded microspheres were added to 30 mL of a KCl/HCl buffer solution of pH 2 at  $37^\circ\text{C}$  and subsequently introduced into a dialysis tube. After being carefully closed, the suspension-filled dialysis tube was fixed at the bottom of a glass reactor with 220 mL of the buffer solution of pH 2 at  $37^\circ\text{C}$ . The external solution was stirred at 120 rpm using a propeller-shaped stirrer with 60 mm of diameter. Then, aliquots of 3 mL were collected from the external solution at specified periods, and then absorption readings were made at 228 nm by means of a UV-vis spectrophotometer (Shimadzu, UV mini 1240). After, the aliquots were brought back into the reactor.

The concentrations of amoxicillin released from the microspheres were determined from an analytical curve correlating the absorption to the concentration of the antibiotic. The square of the linear regression coefficient ( $R^2$ ) was 0.9992. The measures of release were performed without and with the applying of a constant magnetic field of intensity 48 MGOe.

## 2.6. Characterizations

### 2.6.1. $^1\text{H}$ NMR and solid-state $^{13}\text{C}$ -CP/MAS NMR spectroscopies

$^1\text{H}$  NMR and  $^{13}\text{C}$ -CP/MAS NMR spectra were recorded on a Varian spectrometer (model Mercury Plus BB) by applying frequencies of 300.059 MHz and 74.47 MHz for nuclei of  $^1\text{H}$  and  $^{13}\text{C}$ , respectively. To record the  $^1\text{H}$  NMR spectra, 20 mg of the raw or modified pectin were dissolved in 0.7 mL of  $\text{D}_2\text{O}$  containing 0.05% 3-(trimethylsilyl) propionic acid- $\text{d}_4$  sodium salt as an internal reference. The angle pulse and the relaxation time were fixed in  $90^\circ$  and 30 s, respectively. The solid-state  $^{13}\text{C}$ -CP/MAS NMR spectra were obtained using angle pulse of  $37^\circ$ , frequency of 12 kHz, contact time of 3 ms, and relaxation time of 3 s.

### 2.6.2. Scanning electron microscopy (SEM) and energy dispersive spectroscopy (EDS)

Morphological characteristics of the samples were analyzed in a scanning electron microscope (Shimadzu, model SS 550 Superscan) coupled to an energy dispersive spectroscope. The samples were earlier sputter-coated with a thin layer of gold. SEM images were made applying an acceleration voltage of 15 kV and a current intensity of  $30 \mu\text{A}$ . The morphology of  $\text{TiO}_2$  particles was examined in a high resolution Field Emission Scanning Electron Microscope (EOL model 7500 F). A stirred suspension of these particles in ethanol was added dropwise onto a conductor substrate of silicon before visualization by SEM.

### 2.6.3. Measures of dynamic light scattering (DLS) and $\zeta$ -potential

Diluted suspensions of microspheres were prepared with addition of a very small quantity of sample to 1.5 mL of water at room temperature while stirring. After 15 min of dispersion, the suspension became clear because of dilution. Later, the 1.5 mL of the stirred suspension were introduced into a glass cell for

DLS analysis. The diameters of water-dispersed particles were determined from intensity size distributions using a Nano Particle Size and Zeta Potential DLS Analyzer from Particulate Systems. Data were processed with the use of a software supplied by own manufacturer. This apparatus measures  $\zeta$ -potential of particles suspended in a liquid medium. The readings are made with the injection of 0.7 mL into a standard sample flow cell under desired temperature. The values of the  $\zeta$ -potential were recorded at room temperature using stirred suspensions of microspheres.

### 2.6.4. Wide-angle ray-X diffraction (WAXD)

Wide-angle X-rays diffraction (WAXD) patterns were recorded on a Shimadzu Diffractometer model D6000 equipped with a Ni-filtered  $\text{Cu-K}\alpha$  radiation by applying an accelerating voltage of 40 kV and a current intensity of 30 mA. The WAXD data were collected in scale of  $2\theta = 5\text{--}70^\circ$  using a scanning speed of  $2^\circ \text{min}^{-1}$  and a preset time of 0.60 s.

### 2.6.5. Transmission electron microscopy (TEM)

Transmission electron microscopy (TEM) images were obtained on a JEM-1400 microscope (JEOL) by applying an acceleration voltage of 120 kV. For TEM imaging, an aliquot of a stirred suspension of nanoparticles in isopropyl alcohol was added dropwise onto a 400 mesh copper grid covered with a thin layer of carbon.

### 2.6.6. Cytotoxicity assay

VERO cells grown in DMEM plus 10% of fetal bovine serum (FBS) and  $50 \mu\text{g/ml}$  gentamicin were distributed in a 96-well microplate at  $2.5 \times 10^5$  cells/well concentration and incubated in a humid atmosphere with 5%  $\text{CO}_2$  at  $37^\circ\text{C}$  until a confluent monolayer be formed. The medium was then removed, and  $100 \mu\text{L}$  of DMEM was added with different concentrations (1000, 500, 100 and  $10 \mu\text{g mL}^{-1}$ ) of PM0T0 or PM1T1 solutions, in duplicate.

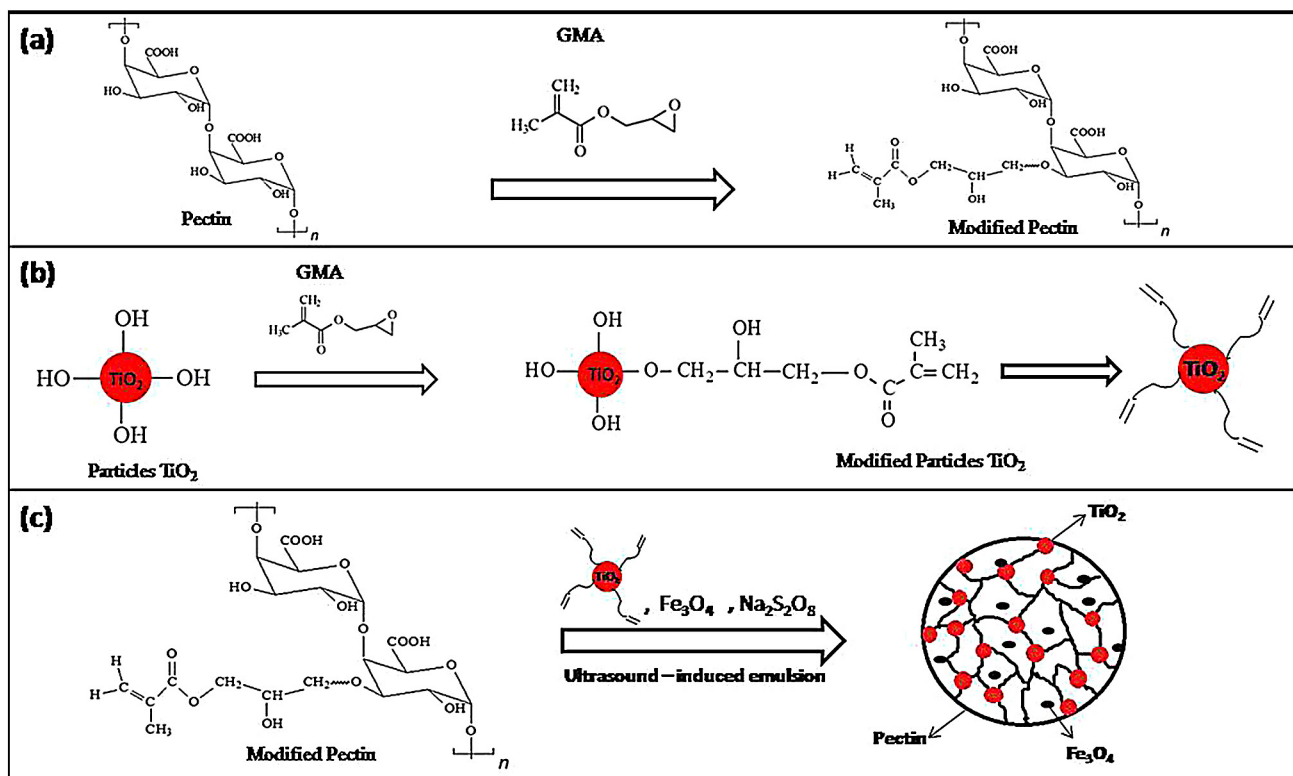


**Fig. 1.** Schema of the preparation of the microspheres: (a) chemical modification of pectin with GMA, (b) chemical modification of  $\text{TiO}_2$  with GMA, and (c) synthesis of  $\text{TiO}_2$ -crosslinked pectin microspheres through ultrasound-induced crosslinking/polymerization in emulsion.

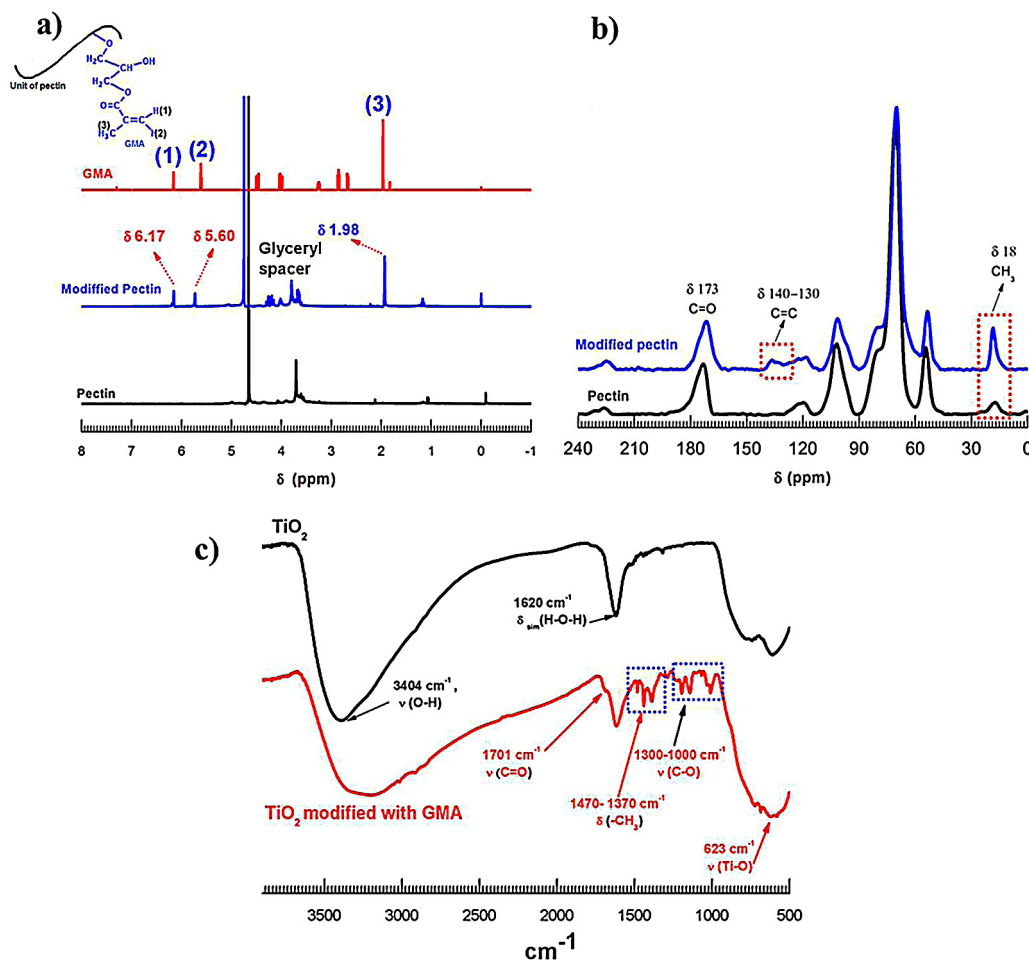


**Fig. 2.**  $^1\text{H}$  NMR spectra of pectin, modified pectin and GMA (a),  $^{13}\text{C}$ -CP/MAS NMR spectra of pectin and modified pectin (b) and FTIR spectra of  $\text{TiO}_2$  and modified  $\text{TiO}_2$  (c).

A control that used cells without the addition of the solutions was also included. The plate was incubated again in a humid chamber at  $37^\circ\text{C}$  with 5%  $\text{CO}_2$  for 72 h. Viable cells were detected using the sulforhodamine B colorimetric method. For this, after culturing, the monolayers were washed with a saline solution of phosphate buffer with pH 7.4 and were fixated using  $50\ \mu\text{L}$  of 10% trichloroacetic acid solution at  $4^\circ\text{C}$  for 1 h. After this, the cells were washed with running water and dried at room temperature. Fifty microliters of sulforhodamine B were added to all of the wells and after a 30-min incubation period at  $37^\circ\text{C}$ , the plates were washed with 1% acetic acid solution three times, and then  $150\ \mu\text{L}$  of 10 mM Tris base were added to each well. Plates were stirred and the optical densities (OD) were read at 530 nm in an ELISA reader (Bio-Tek FL-600 Microplate Fluorescence Reader), and the cytotoxic concentration for 50% of VERO cells ( $\text{CC}_{50}$ ) was determined through linear regression.

### 3. Results and discussion

#### 3.1. Modification of pectin and $\text{TiO}_2$ with GMA

Fig. 2(a) shows the  $^1\text{H}$  NMR spectra of pectin, modified pectin and GMA. The signals at  $\delta$  6.17 and  $\delta$  5.60 in the spectrum of modified pectin are associated to vinyl carbon-linked hydrogen and the signal at  $\delta$  1.98 was attributed to hydrogen of methyl groups at the vinyl carbons. These signals indicate the attachment of chemical groups derived from GMA to pectin. In the solutions with pH 3.5, which was the pH of the reaction medium, GMA reacts with

carboxylic and/or hydroxyl groups of the polysaccharide by an epoxide ring-opening mechanism route. The appearance of corresponding signal of GMA-derived glyceryl spacer in the spectrum of modified pectin is a strong evidence of the occurrence of such a mechanism. The great advantage of pectin, from the chemical point of view, is that it has both carboxylic and hydroxyl groups along its structure.

Fig. 2(b) shows the  $^{13}\text{C}$ -CP/MAS NMR spectra of pectin and modified pectin. The signal that appears in spectral region of  $\delta$  140–130 in the spectrum of modified pectin was ascribed to vinyl carbons derived from GMA. The increase in the intensity of the signal at  $\delta$  18, in the same spectrum, was corresponded to an increase of methyl carbons in the modified pectin. The data found in both spectroscopic techniques give an overview of the modification of pectin with GMA.

Fig. 2(c) shows the FTIR spectra of  $\text{TiO}_2$  and modified  $\text{TiO}_2$ . The band at  $3404\ \text{cm}^{-1}$  in the spectrum of  $\text{TiO}_2$  was assigned to stretching vibrations of O–H bonds and the band at  $1620\ \text{cm}^{-1}$  was attributed to H–O–H bending. Both bands are the result of water adsorbed on  $\text{TiO}_2$  particles. In both spectra, there is a band at approximately  $623\ \text{cm}^{-1}$  that corresponds to stretching vibrations of structural Ti–O on  $\text{TiO}_2$  particle.

The bands in the spectral regions of  $1701\ \text{cm}^{-1}$  (C=O stretching vibrations),  $1470$ – $1370\ \text{cm}^{-1}$  (asymmetric C–H and symmetric C–H bending of terminal  $\text{CH}_3$  groups), and  $1300$ – $1000\ \text{cm}^{-1}$  (C–O stretching vibrations) that appear in the spectrum of modified  $\text{TiO}_2$  are derived from GMA, indicating the modification of  $\text{TiO}_2$ . The stretching band that refers to C=C groups of GMA was not

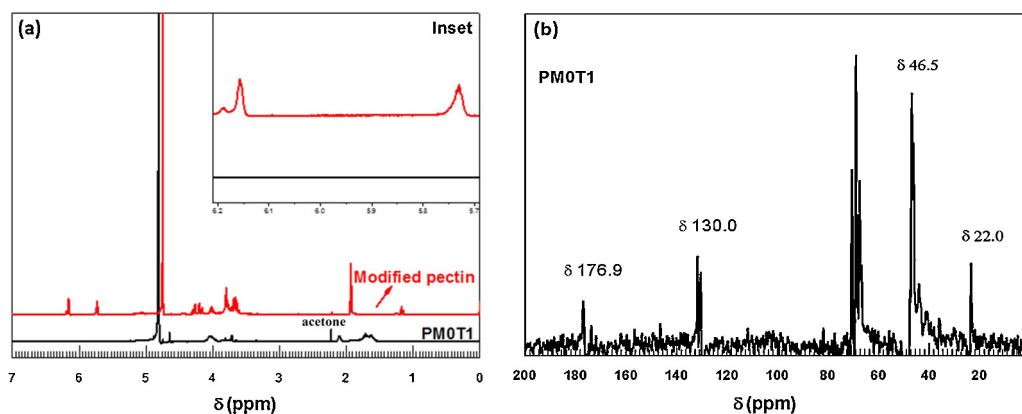


**Fig. 3.**  $^1\text{H}$  NMR spectra of modified pectin and PMOT1 (a) and  $^{13}\text{C}$  NMR spectrum of PMOT1 (b). Inset of (a) shows magnification of the region of 5.7–6.2 ppm in which spectral significant changes can be observed.

observed, because it is covered by the broad band of adsorbed water.

### 3.2. Nanostructured pectin microspheres

Fig. 3(a) shows the  $^1\text{H}$  NMR spectra of modified pectin and PMOT1. The signal corresponding to  $^1\text{H}$  nucleus of acetone, which was the solvent used for particle precipitation, was detected in the spectrum of PMOT1. The signals at  $\delta$  6.17 and  $\delta$  5.60 in the spectrum of modified pectin are attributed to the *cis* vinyl hydrogen derived from GMA. The disappearance of such signals in the spectrum of PMOT1 indicates the consumption of the carbon–carbon double bonds during the crosslinking/polymerization reaction. This finding is confirmed by the  $^{13}\text{C}$  NMR spectrum (Fig. 3(b)) in which the signals that refer to vinyl carbon groups ( $\text{C}=\text{C}$ ) were absent.

Although the microspheres were separated from the emulsion by centrifugation at 7000 rpm, washed with ethanol and acetone (three times in each), the signals at  $\delta$  130.0 (benzyl alcohol) and  $\delta$  46.5 (PVA) were still observed.

Fig. 4 shows the SEM images and EDS curves of PMOT0, PMOT1, PM1T0 and PM1T1. The SEM images show microspheres with well-defined spherical shape. Such architecture was formed through the crosslinking/polymerization reaction of modified pectin at the interior of the alcohol-confined water droplets under ultrasound. In other words, the spherical form of the microparticles results of a macromolecular fine-tuning of hydrophilic chains of pectin to water droplets during the reaction.

The presence of the inorganic elements, such as Fe and Ti, in the samples was detected by EDS analysis. Fe was observed in PM1T0 and PM1T1, and Ti was detected in PMOT1 and PM1T1, even after the samples were centrifuged at 7000 rpm and repeatedly washed with ethanol and acetone.

Fig. 5 shows the intensity size distribution and  $\zeta$ -potential curves of PMOT0, PMOT1, PM1T0 and PM1T1. The particle size distribution curves showed maxima at 416 nm for PMOT0, at 514 nm for PMOT1, at 889 nm for PM1T0, and at 675 nm for PM1T1. The introduction of  $\text{Fe}_3\text{O}_4$  and/or  $\text{TiO}_2$  produced pectin microspheres with a larger average diameter. It is important to report that the term introduction was used in a contextualized way to refer  $\text{Fe}_3\text{O}_4$  and/or  $\text{TiO}_2$  within the pectin microspheres, because  $\text{TiO}_2$  was indeed used as a crosslinker agent.

The presence of these particles in the microspheres, as demonstrated using EDS, is the result of physical and/or chemical interactions between the inorganic substances and pectin, providing new bonds that could change the negative charges of the

microspheres, because of anionic groups of the polysaccharide. Consequently, the  $\zeta$ -potentials of microspheres could change with introduction of  $\text{Fe}_3\text{O}_4$  and/or  $\text{TiO}_2$ . The  $\zeta$ -potentials of microspheres in water were obtained as follows:  $\zeta = -29.46$  mV for PMOT0,  $\zeta = -9.54$  mV for PMOT1,  $\zeta = -7.86$  mV for PM1T0, and  $\zeta = -4.87$  mV for PM1T1. The  $\zeta$ -potentials became less negative in the microspheres with  $\text{Fe}_3\text{O}_4$  and/or  $\text{TiO}_2$  added, probably caused by presence of both inorganic particles in the negatively charged pectin. This effect was prominent for  $\text{Fe}_3\text{O}_4$  (PM1T0), compared to  $\text{TiO}_2$  (PMOT1), although the introduction of both substances significantly changed the  $\zeta$ -potential from  $-29.46$  mV to  $-4.87$  mV.  $\text{Fe}_3\text{O}_4$  interacts with pectin microspheres by complexation of iron ions from the mineral with carboxyl groups from polysaccharide [21] and neutralizes somewhat the negative electric charges on microsphere surface. Furthermore, the  $\text{Fe}_3\text{O}_4$  particles appear to behave as a cationic stabilizer for negatively charged compounds, as pectin, *via* an electrostatic complexation. In the case of Ti, the data of  $\zeta$ -potential corroborate the analysis of FTIR (Fig. 2(c)), which is an indicative of the reaction of modified  $\text{TiO}_2$  with modified pectin.

Fig. 6 shows the WAXD patterns of  $\text{Fe}_3\text{O}_4$ , modified  $\text{TiO}_2$  and pectin microspheres. In Fig. 6(c), a crystalline plan diffraction signal was found at approximately  $35^\circ$  ( $220$ ), corresponded to that of  $\text{Fe}_3\text{O}_4$  (Fig. 6(a)), for PM1T0 and PM1T1 microspheres. The absence of WAXD signals of Ti in the diffractograms of Fig. 6(c) were attributed to main factors: (i) low amount of  $\text{TiO}_2$  and (ii) WAXD signals of low intensity. The signal of higher intensity in the diffractogram of  $\text{TiO}_2$  (Fig. 6(b)), ascribed to crystalline plan (1 0 1), is covered by the large amorphous signal of pectin, shown in Fig. 6(c).

Fig. 7 shows the TEM images of pectin microspheres. Two distinct phases displaying defined forms were observed: one brightest-imaged and the other darkest-imaged. The appearance of such phases depends on the atomic number of the elements in the sample. The light atoms, those that has a small molar mass, difficult the scattering of electrons and thus there is no separation (definition) between the darkest and brightest areas of the image. The light atoms of carbon, hydrogen and oxygen, which constitute the polysaccharide structure of pectin, correspond to brightest areas. In both images, the largest sphere-shaped areas were assigned to pectin. The heavy atoms, such as Fe and Ti, allow a better contrast and correspond to darkest areas. Nanostructures with defined forms are observed within the pectin microsphere. The nanostructures that appear in the TEM images of Fig. 7(a) were attributed to  $\text{TiO}_2$  because, obviously, there is no  $\text{Fe}_3\text{O}_4$  in PMOT1. Similarly, the nanostructures in Fig. 7(b) correspond to  $\text{Fe}_3\text{O}_4$  because PM1T0 does not contain  $\text{TiO}_2$ .

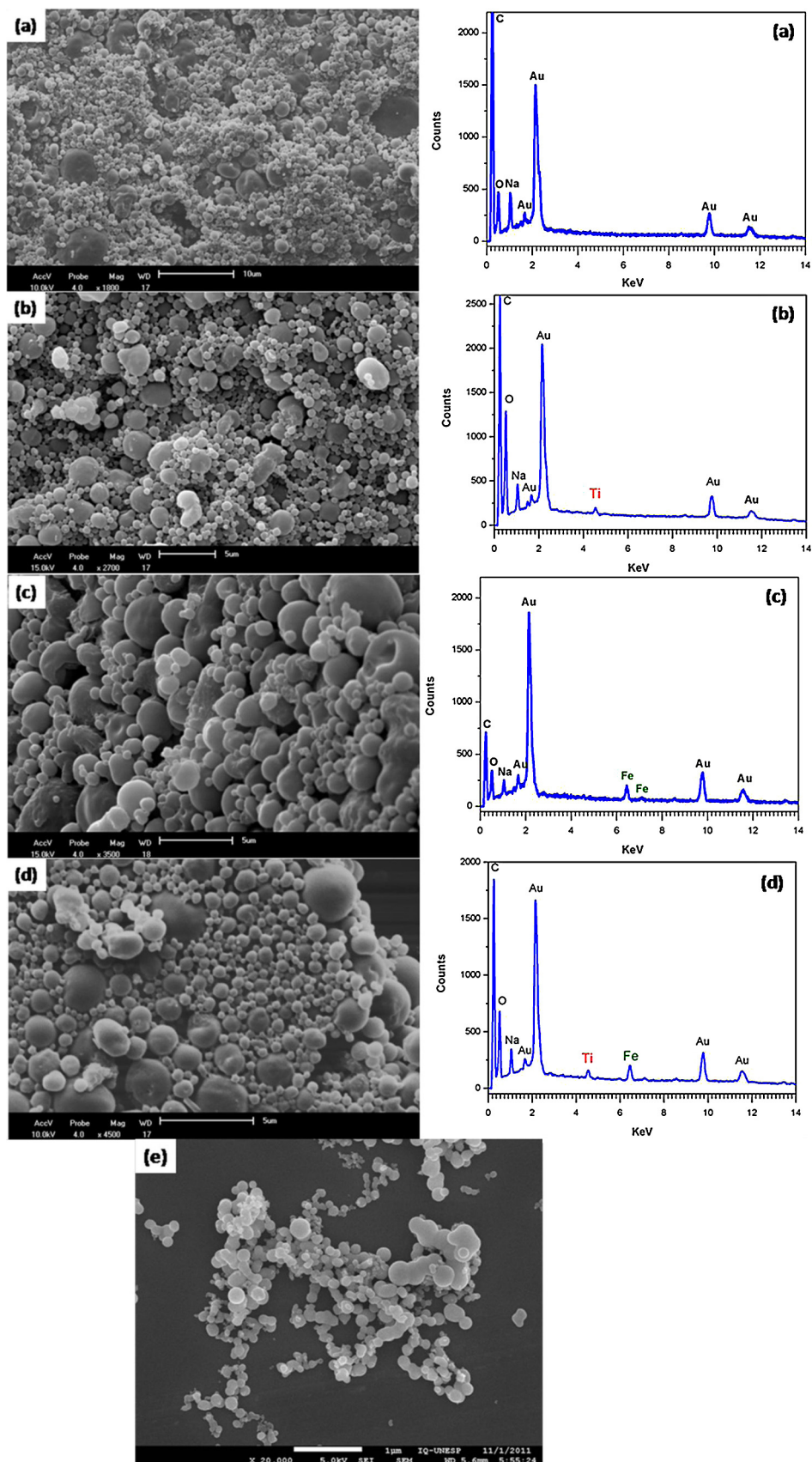


**Fig. 4.** SEM images (right) and EDS curves (left) of PM0T0 (a), PM0T1 (b), PM1T0 (c), PM1T1 (d), and TiO<sub>2</sub> particles (e). SEM image of TiO<sub>2</sub> particles was taken in a high resolution field emission scanning electron microscope.

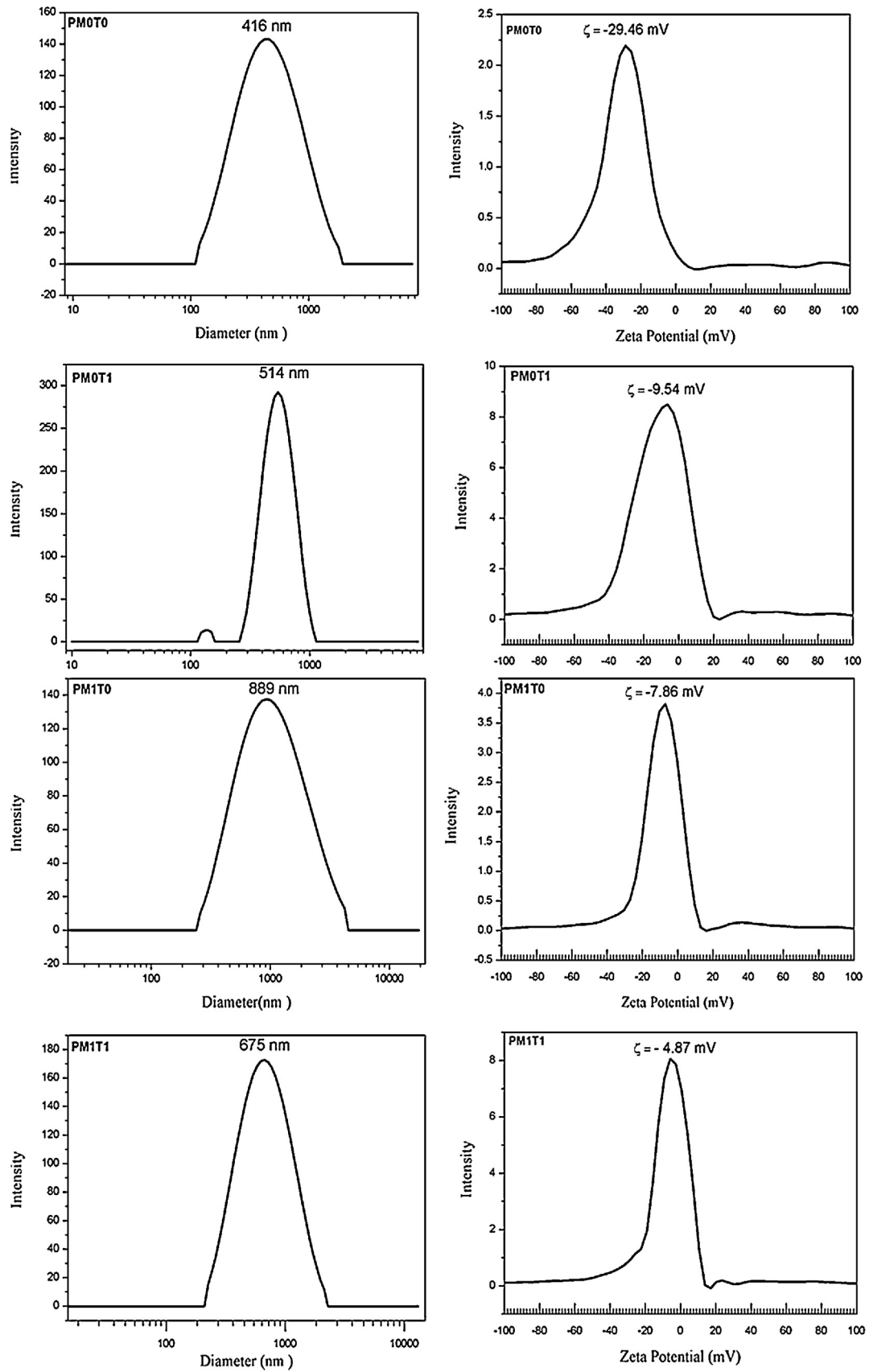


Fig. 5. Particle size distribution ((DLS) left) and  $\zeta$ -potential curves (right) of PM0T0, PM0T1, PM1T0, and PM1T1.

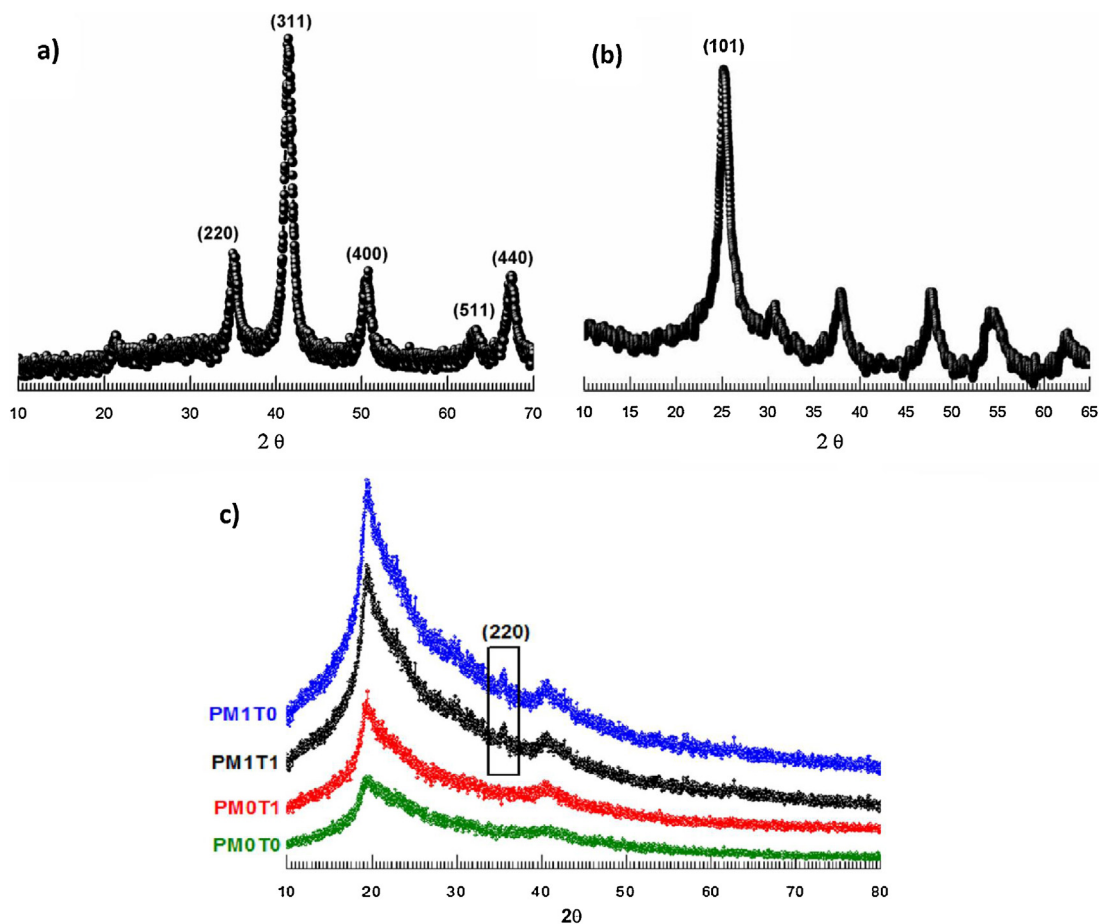


Fig. 6. Wide-angle X-ray diffraction patterns of magnetite (a), modified  $\text{TiO}_2$  (b) and pectin microspheres (c).

### 3.3. Amoxicillin release from the microspheres in the acid medium

Fig. 8 shows the time-dependent release curves of amoxicillin from PMOT0, PMOT1, PM1T0 and PM1T1 without and with an applied magnetic field at  $37^\circ\text{C}$ . PMOT0, which is the reference sample, showed higher amoxicillin release. With the introduction of  $\text{Fe}_3\text{O}_4$  and/or  $\text{TiO}_2$  to the microspheres, the concentrations of the released antibiotic reduced with time. On the other hand, the

levels of the drug in the acid medium are sustained throughout the experiment. The concentrations of the antibiotic slowly increased in approximately 2–3 h of release, which is the time taken for food to transit throughout the stomach, and kept invariable in the period of 3–5 h.

The mass percentages of loaded antibiotic on the microspheres before the measures of release were 94% for PMOT0, 89% for PMOT1, 79% for PM1T0, 82% for PM1T1. Although the ethanol is

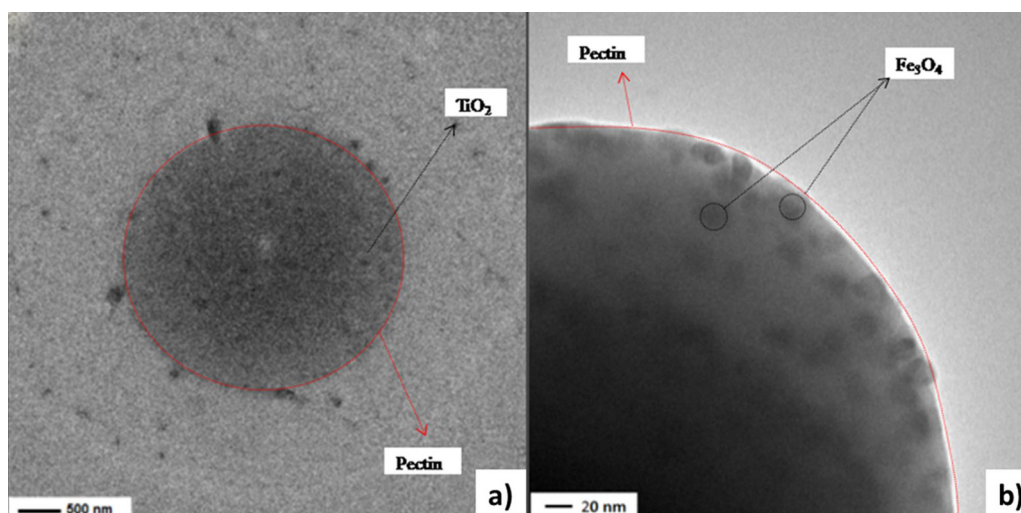
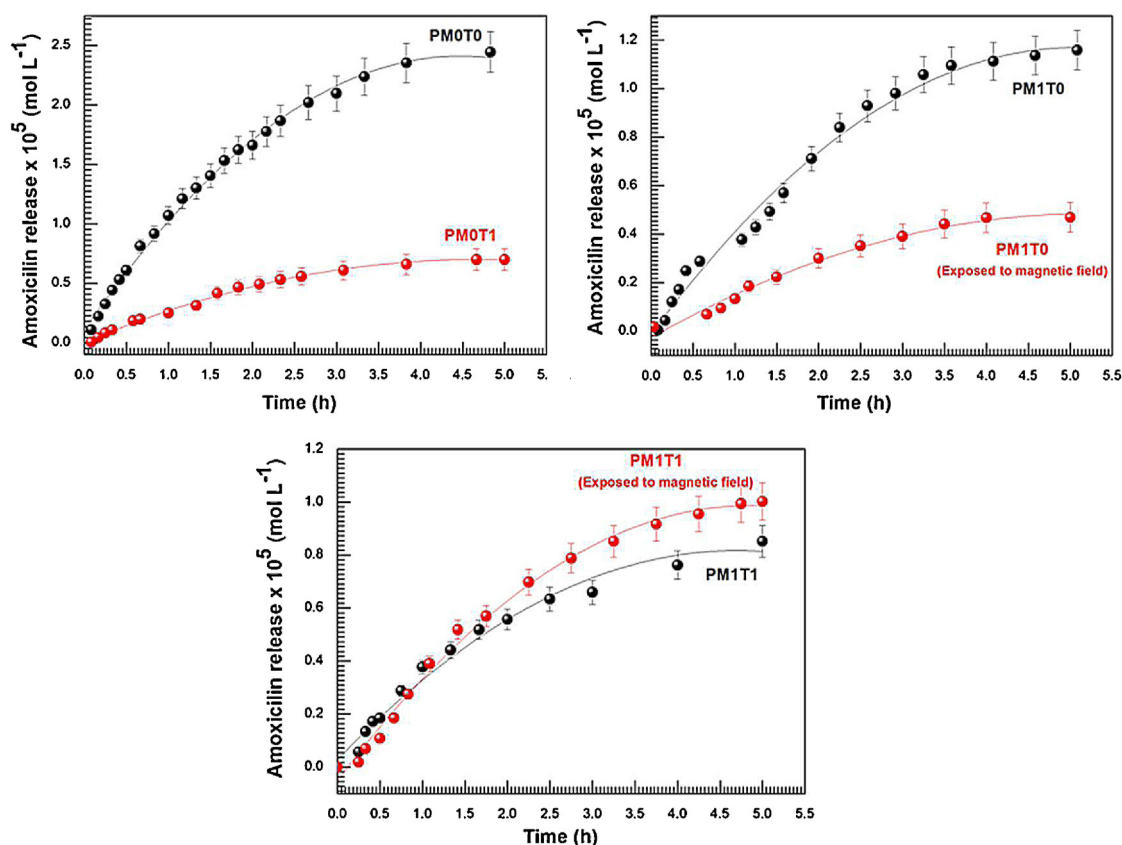


Fig. 7. Transmission electron microscopy (TEM) images of pectin microspheres: PMOT1 (a) and PM1T0 (b).



**Fig. 8.** Time-dependent release curves of amoxicillin from PMOT0, PMOT1, PM1T0 and PM1T1 without and with an applied magnetic field at 37 °C. The effect of the magnetic field on the antibiotic release was determined with the applying of a homogenous magnetic field of intensity 48 MGOe.

a good solvent for amoxicillin, pectin is highly insoluble in an alcoholic environment. In the pectin precipitated microspheres the movement of matter through them, which occurs by a diffusive mechanism, is expressively minimized or null, preventing the release of the antibiotic.

The mass percentages of antibiotic released after 5 h of experiment were 34.5% for PMOT0, 6.4% for PMOT1, 11.1% for PM1T0, and 7.2% for PM1T1. When the magnetic field is on, there is a significant reduction in the release: PMOT1 (4.7%) and PM1T1 (8%). In the microparticles with Fe<sub>3</sub>O<sub>4</sub> and/or TiO<sub>2</sub>, the release is slower than in the pectin-only microparticles (PMOT0) owing to a tortuosity effect, as a result of the disposition of Fe<sub>3</sub>O<sub>4</sub> and/or TiO<sub>2</sub> in the microparticle. The difference between the loaded antibiotic and released antibiotic amounts was attributed to a partitioning effect. Partition is the result of physical chemical affinities between the microspheres and the surrounding liquid. In other words, the interactions between the pectin and the amoxicillin hinder the total release of the loaded drug.

The effect of the magnetic field on the release can be better understood when it is related to diffusional laws. The diffusional properties of a certain device can be determined by Eq. (1) [22]. The diffusional coefficient,  $n$ , has been often used to interpret the release profile of a given solute from a polymer network.

$$\frac{w_t}{w_{eq}} = kt^n \quad (1)$$

here,  $w_t$  and  $w_{eq}$  are the weights of solute released from the microspheres at a specified time and at equilibrium, respectively, and  $k$  is a constant characteristic of the network structure.

Eq. (1) can predict only the first 60% of released solute. The  $n$  parameter has different conceptual meanings depending on geometrical shape of the material. For sphere, which is the geometry

**Table 1**

$R$ -square ( $R^2$ ) and diffusional exponent  $n$ , according to Eq. (1), of amoxicillin release for pectin microspheres of different compositions without and with an applied magnetic field.

Microsphere composition	Diffusional exponent $n$	
	Without applying a magnetic field	With an applied magnetic field
PMOT0	1.15 ( $R^2 = 0.99$ )	–
PMOT1	0.96 ( $R^2 = 0.99$ )	–
PM1T0	1.01 ( $R^2 = 0.95$ )	0.93 ( $R^2 = 0.99$ )
PM1T1	0.94 ( $R^2 = 0.95$ )	0.87 ( $R^2 = 0.95$ )

of pectin microparticles,  $n$  has the following meanings: (i)  $n = 0.43$  for Fickian diffusion (Case I), (ii)  $0.43 < n < 0.85$  for anomalous transport, contribution of Fickian diffusion and controlled relaxation, (iii)  $n = 0.85$  for zero order (Case II), and (iv)  $n > 0.85$  for super Case II, contribution of the macromolecular relaxation of the polymer chains. The values of  $n$  were obtained from slopes of the logarithmic curves of release ( $w_t/w_{eq}$ ) ratio plotted against  $t$ , and the data were shown in Table 1.

The amoxicillin release mechanism of PMOT0 is governed by macromolecular relaxation. With the introduction of Fe<sub>3</sub>O<sub>4</sub> and/or TiO<sub>2</sub>, the antibiotic release is also driven by macromolecular relaxation of the pectin chains. However, there is a tendency to anomalous transport. In such a case, the release is disturbed by both a reduction in the polymer motion that affects the relaxation mechanism and the tortuosity effect. When the magnetic field is on, the amoxicillin release became more dependent on the anomalous transport because of an additional decrease in the polymer motion of the network structure of pectin, providing a larger extent release profile (sustained release). This means that the antibiotic release

may possibly be modulated by exposition of the magnetic pectin microspheres to a remote magnetic field, which would allow prevention of the premature release of the drug. In practical terms, the nanostructured microspheres, under a magnetic field, could deliver a larger proportion of their initial load to specific site of action. Although the stomach offers a narrow therapeutic window for many antibiotics, the pectin microspheres showed a sustained release rate of amoxicillin in the acid medium.

#### 3.4. Cytotoxicity evaluation

*In vitro* cytotoxicity assay, which is a standardized approach to analyze both biocompatibility and toxicity of materials, was performed to evaluate the pharmacological potential of the prepared microspheres. The cytotoxic concentrations for 50% of VERO cells ( $CC_{50}$ ), calculated as the concentration required to reduce cell viability by 50% after 72 h of incubation, for PM0T0 and PM1T1 were  $217.7 \pm 6.5$  and  $121.5 \pm 4.9 \mu\text{g mL}^{-1}$ , respectively. Although the cytotoxic risk increased with addition of both  $\text{Fe}_3\text{O}_4$  and  $\text{TiO}_2$  to pectin microspheres, the  $CC_{50}$  values are quite interesting for an incubation time of 72 h, showing an acceptable biocompatibility.

#### 4. Conclusions

$\text{TiO}_2$ -crosslinked pectin microspheres with  $\text{Fe}_3\text{O}_4$  particles were prepared using a nanostructuring approach based on a water-in-oil emulsion. The presence of these particles in the microspheres is the result of physical and/or chemical interactions between the inorganic substances and pectin. The  $\zeta$ -potentials became less negative in the microspheres with  $\text{Fe}_3\text{O}_4$  and/or  $\text{TiO}_2$  added, likely caused by presence of the inorganic particles in the negatively charged pectin.

The mass percentages of loaded antibiotic on the microspheres before the measures of release were 94% for PM0T0, 89% for PM0T1, 79% for PM1T0, 82% for PM1T1. The mass percentages of antibiotic released after 5 h of experiment were 34.5% for PM0T0, 6.4% for PM0T1, 11.1% for PM1T0, and 7.2% for PM1T1. With an applied magnetic field, there was a significant reduction in the release: PM0T1 (4.7%) and PM1T1 (8%). The nanostructured pectin microspheres showed an amoxicillin release rate slower than that of the pure pectin microspheres. On the other hand, the levels of the drug in the acid medium were sustained throughout the experiment. The amoxicillin release mechanism of the pure pectin microsphere is governed by macromolecular relaxation. In the structured microspheres, the antibiotic release is also driven by macromolecular relaxation of the pectin chains. However, there is a tendency to anomalous transport. In such a case, the release is disturbed by both a reduction in the polymer motion that affects the relaxation mechanism and the tortuosity effect. When the magnetic field is on, the amoxicillin release became more dependent on the anomalous transport because of an additional decrease in the

polymer motion of the network structure of pectin, providing a larger extent release profile. This means that the antibiotic release may possibly be modulated by exposition of the magnetic pectin microspheres to a remote magnetic field, which would allow prevention of the premature release of the drug. In practical terms, the nanostructured microspheres, under a magnetic field, could deliver a larger proportion of their initial load to specific site of action. Although the stomach offers a narrow therapeutic window for many antibiotics, the pectin microspheres showed a sustained release rate of amoxicillin in the acid medium. The cytotoxic concentrations for 50% of VERO cells ( $CC_{50}$ ), for PM0T0 and PM1T1 were  $217.7 \pm 6.5$  and  $121.5 \pm 4.9 \mu\text{g mL}^{-1}$ , respectively. The  $CC_{50}$  values showed acceptable biocompatibility for pectin microspheres, even after the introduction of  $\text{TiO}_2$  and  $\text{Fe}_3\text{O}_4$ .

#### Acknowledgments

E.P.P. and D.L.A.S. thank the Coordenação de Aperfeiçoamento de Pessoal de Nível Superior (CAPES) for doctorate fellowship. M.R.G. thanks the CAPES/PNPD for post-doctorate fellowship. M.R.M. thanks the Conselho Nacional de Desenvolvimento Científico e Tecnológico (CNPq). A.F.R. and M.H.K. acknowledge the financial supports given by CNPq, CAPES, Instituto de Ciência, Tecnologia e Inovação em Materiais Complexos Funcionais (INOMAT) and Fundação Araucária-Brasil.

#### References

- [1] J. Shi, Z. Zhang, W. Qi, S. Cao, *Int. J. Biol. Macromol.* 50 (2012) 747–753.
- [2] G. Li, S. Song, T. Zhang, M. Qi, J. Liu, *Int. J. Biol. Macromol.* 62 (2013) 203–210.
- [3] G. Li, L. Guo, Q. Wen, T. Zhang, *Int. J. Biol. Macromol.* 55 (2013) 69–74.
- [4] S. Parveen, R. Misra, S.K. Sahoo, *Nanomed.: Nanotechnol. Biol. Med.* 8 (2012) 147–166.
- [5] S. Patil, S. Gawali, S. Patil, S. Basu, *J. Mater. Chem. B* 1 (2013) 5742–5750.
- [6] A. Gautam, F.C.J.M. van Veggel, *J. Mater. Chem. B* 1 (2013) 5186–5200.
- [7] D. Maity, D.C. Agrawal, *J. Magn. Mater.* 308 (2007) 46–55.
- [8] Q. Yuan, R. Venkatasubramanian, S. Hein, R.D.K. Misra, *Acta Biomater.* 4 (2008) 1024–1037.
- [9] G. D'Ayala, M. Malinconico, P. Laurienzo, *Molecules* 13 (2008) 2069–2106.
- [10] F. Munarin, P. Petrini, M.C. Tanzi, M.A. Barbosa, P.L. Granja, *Soft Matter* 8 (2012) 4731–4739.
- [11] T. Katav, L. Liu, T. Traitel, R. Goldbart, M. Wolfson, J. Kost, *J. Control. Release* 130 (2008) 183–191.
- [12] L. Liu, M. Fishman, K. Hicks, *Cellulose* 14 (2007) 15–24.
- [13] M.J. Fernández-Hervás, J.T. Fell, *Int. J. Pharm.* 169 (1998) 115–119.
- [14] L. Liu, M.L. Fishman, J. Kost, K.B. Hicks, *Biomaterials* 24 (2003) 3333–3343.
- [15] V.R. Sinha, R. Kumria, *Int. J. Pharm.* 224 (2001) 19–38.
- [16] S.T. Charlton, S.S. Davis, L. Illum, *J. Control. Release* 118 (2007) 225–234.
- [17] L. Joergensen, B. Klösgen, A.C. Simonsen, J. Borch, E. Hagesaether, *Int. J. Pharm.* 411 (2011) 162–168.
- [18] A. Kaur, G. Kaur, *Saudi Pharm. J.* 20 (2012) 21–27.
- [19] P. Sriamornsak, N. Wattanakorn, H. Takeuchi, *Carbohydr. Polym.* 79 (2010) 54–59.
- [20] L. Ferreira, M.M. Vidal, C.F.G.C. Geraldes, M.H. Gil, *Carbohydr. Polym.* 41 (2000) 15–24.
- [21] E. Kroll, F.M. Winnik, R.F. Ziolo, *Chem. Mater.* 8 (1996) 1594–1596.
- [22] P.L. Ritger, N.A. Peppas, *J. Control. Release* 5 (1987) 37–42.